AMSI VACATION RESEARCH SCHOLARSHIPS 2018-2019

Optimal cruise control with dual electric motors

Thomas Miller

Supervised by Peter Pudney & Peng Zhou
University of South Australia

Vacation Research Scholarships are funded jointly by the Department of Education and Training and the Australian Mathematical Sciences Institute.

AMSI AUSTRALIAN MATHEMATICAL SCIENCES INSTITUTE

Australian Government
Department of Education and Training

Abstract

The ATN group of universities is building a solar car to participate in the 2019 World Solar Challenge. The car will have two identical electric motors—one on each of the rear wheels. Each motor has a associated motor controller that controls the current applied to the motor windings, and hence the torque of the motor. The motors and motor controllers have efficiencies that depend on parameters including speed, current, torque and temperature.

When the car is cruising at a constant speed, the torque required to maintain the required speed will depend on external forces including aerodynamic drag, wind forces and the gradient of the road. Usually, the total torque required will be less than the capability of a single motor. The aim of the research is to determine how much total torque is required to maintain a constant speed, and how much of this total torque should be generated from each motor to minimise the sum of the power losses in the motors and controllers. For some conditions, the optimal control might be to generate the same torque from both motors, whereas for different conditions it might be more efficient to generate all of the torque from one motor.

The motor manufacturer provides information that can be used to model the efficiency of the motor, which depends on torque and angular velocity. The controller manufacturer provides an efficiency map for the controller; controller efficiency also depends on torque and angular velocity.

We show that the power losses are minimised if the same torque is applied to both motors.

1 Introduction

In the World Solar Challenge, when a car leaves Darwin on the 3,000 km journey to Adelaide it starts with only about one tenth of the energy required to make it to the end. The rest of the energy is provided by the sun [World Solar Challenge, 2019]. Solar cars make this journey with far less energy than a commercial automobile requires [Thacher, 2015]. To make this possible, solar cars must be as efficient as possible by minimising the energy losses that occur during the journey.

The Australian Technology Network (ATN) group of universities are building a solar car (Figure 1) to compete in the 2019 World Solar Challenge. This solar car will be powered by two in-wheel motors, each controlled by an associated motor controller. The roads from Darwin to Adelaide are mostly long and straight allowing the car to spend most of the journey cruising at a constant speed.

Figure 1: The ATN Solar Car

The aim of this project is to analyse the losses that occur in the motors and controllers at cruising speed and propose a simple real-time control strategy that minimises the energy lost at this speed.

2 Modelling

The factors that influence losses in the motor and controller at cruising speed are:

- the rotational speed of the motors
- the torque required to maintain cruising speed
- the DC bus voltage that the battery provides to the system
- the ambient temperature around the motors.

The cruising speed v of the car will be 75 km/h. As the motors are in the wheels, the rotational speed of the motors at cruising speed (measured in radians per second) is determined by the cruising speed and the radius of the tyres, which is 0.2792 meters. To convert from km/h to radians per second (rad/s) we first convert to m/s by dividing by 3.6 so 75 km/h = 75/3.6 m/s, then to get to rad/s we divide this value by the tyre radius giving us $\omega = (75/3.6)/0.2792 \approx 74.62$ rad/s.

The torque τ required to maintain cruising speed depends on the tractive force F required to maintain cruising speed and the radius r of the wheels, and is given by $\tau = Fr$. The tractive force is approximately

$$F \approx c_{\mathrm{rr}} mg + \frac{1}{2} c_{\mathrm{d}} A \rho v^2 + mg \sin\theta.$$

The term $c_{\mathrm{rr}} mg$ is the rolling resistance caused by forces between the wheels and the road, and depends on the rolling resistance coefficient of the tyres c_{rr}, and the load on the wheels mg which depends on the mass of the car m and the experienced gravitational force g. The term $\frac{1}{2} c_{\mathrm{d}} \rho v^2 A$ is the aerodynamic drag experienced by the car and depends on the air density ρ, the drag coefficient of the car c_{d} the reference area of the car A and the square of the car's velocity. The final term is $mg \sin\theta$ and represents the force on the car due to the gradient of the road.

In our case we have:

- $m = 410$ kg (with two occupants)
- $g = 9.8\,\mathrm{m\,s}^{\ 2}$
- $c_{\mathrm{rr}} = 0.005$
- $\rho = 1.16\,\mathrm{kg\,m}^{\ 3}$
- $c_{\mathrm{d}} A = 0.16\,\mathrm{m}^3$
- $v = 75$ km/h ≈ 21 m/s
- $\sin\theta$ as high as 0.06.

For a flat road this means we will need a force of approximately 61 N to maintain a speed of 75 km/h, and for a steep uphill section a force of 302 N is required. These forces correspond to torques of 17 Nm and 84 Nm respectively.

The input voltage to the controller, V_{bus}, will vary from 114 V when the battery is empty to 160 V when the battery is full. Nominally we expect the voltage will be 141 V. We will model the problem firstly with the nominal voltage but also examine how the loses change as this voltage changes.

Finally for the ambient temperature we will assume an average of 35°C (308 K), and we will also examine how the loses change as the ambient temperature changes.

The above parameters are the inputs of our problem. We wish to find how to distribute the required torque between the two motors in order to minimise the total power losses in the motors and motor controllers. The outputs we will produce are:

- the torque provided by motor one
- the torque provided by motor two
- the total power lost by the system.

To solve the problem we must consider losses in three different components of the drive system:

- the motors
- the motor controllers
- the three inductors used between each controller and the corresponding motor.

3 The Motors

The motors to be used in the ATN solar car are two identical Axial Flux Stub Axle Wheel Motors, built by Marand. The motors were designed by the CSIRO for use by the Aurora solar car team for the 1996 World Solar Challenge from Darwin to Adelaide [Lovatt et al., 1998]. Appendix A shows the specifications for the motors.

They are permanent magnet synchronous motors, which is a type of motor that gives the benefits of both a high torque density and high efficiency. The losses that arise from the motors are [Thacher, 2015]:

- copper losses, which are the dominant loss in this motor and are caused by resistance to the flow of current in the motor
- eddy current losses, because the rotation of the motor induces small circulating currents in the motor that impede the motors rotation
- windage losses due to aerodynamic drag resistance to the rotation to the motor caused by air contained in the motor.

Figure 2 shows how these losses vary with torque. Copper loss is the main source of loss in this motor and increases at an increasing rate as torque increases, while eddy and windage losses are almost negligible and are practically independent of torque.

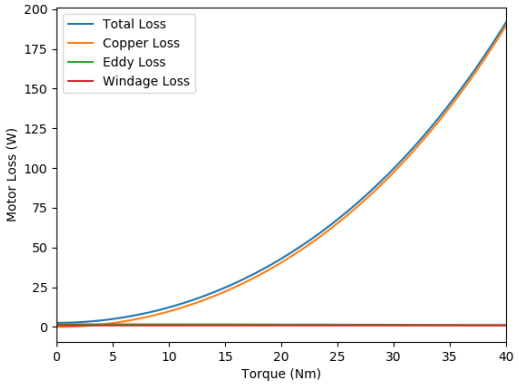

Figure 2: How the Motor Loses Change with Torque

The copper loss and eddy loss are calculated in an iterative process. This process depends on the ambient temperature T_a in K, the motor torque τ in Nm, the motor speed ω in rad/s and requires an estimate of the steady state winding temperature T_w in K [Mar, 2013].

1. The magnet temperature T_m is calculated as approximately halfway between the ambient and winding temperatures: $T_\mathrm{m} = (T_\mathrm{a} + T_\mathrm{w})/2$.
2. The magnet remanence B is given by: $B = 1.32 - 1.2 \times 10^{-3}(T_\mathrm{m} - 293)$.
3. The RMS per phase motor current i is given by: $i = 0.561 B\tau$.
4. The per phase motor winding resistance R is given by: $R = 0.0575\,(1 + 0.0039\,(T_\mathrm{w} - 293))$.
5. The copper loss P_c is given by: $P_c = 3i^2R$.
6. The motor eddy current loss P_e is given by: $P_\mathrm{e} = \left(9.602 \times 10^{-6}(B\omega)^2\right)/R$.
7. The winding temperature T_w is then given by: $T_\mathrm{w} = 0.455(P_\mathrm{c} + P_\mathrm{e}) + T_\mathrm{a}$.
8. The calculations (1)–(7) are repeated the process until the difference between the previous and next winding temperature is less than 0.05 K.

Testing showed that these calculations are accurate to within 5% when the torque is in the range $[0, 40]$ Nm [Mar, 2013].

The other loss associated with the motor is the internal windage loss P_w which is given by [Mar, 2013]:

$$P_\mathrm{w} = 170.4 \times 10^{-6}\omega^2.$$

The total motor loss P_{ml} is the summation of the three individual losses:

$$P_\mathrm{ml} = P_\mathrm{c} + P_\mathrm{e} + P_\mathrm{w}.$$

4 The Controllers

Each motor has an associated motor controller that takes high voltage DC power from the car's batteries and converts it to a lower voltage 3-phase AC power to drive the motor [Tri, 2015]. In our solar car we are using Tritium WaveSculptor 22 motor controllers.

There are two types of losses associated with the motor controller [Tri, 2015]:

- conduction losses, like copper losses, are incurred due to the resistance of current flowing through the motor controller
- switching losses, associated with the switching of the battery voltage that controls the current flowing through the motor phase windings Thacher [2015].

The controller losses are dependent on current which, as shown in Section 3, is proportional to the torque produced by the motor. Figure 3 shows the controller losses. Controller losses are generally lower then the motor losses shown in Figure 2. Both the switching losses and the conduction loss provide a significant contribution to the total controller loss, although the conduction loss is the only loss that is increasing at an increasing rate.

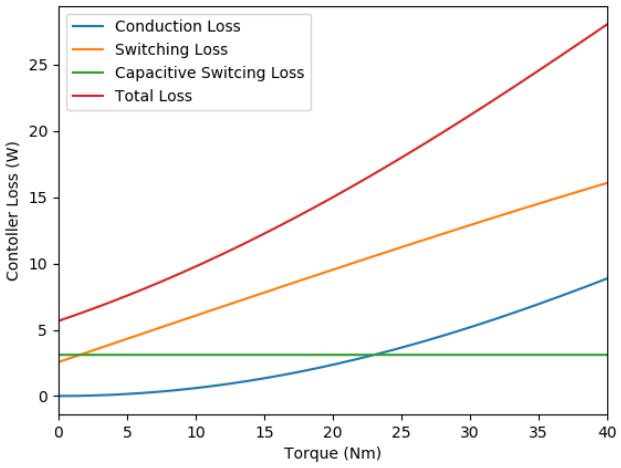

Figure 3: Controller Losses

Simple equations exist for estimating the controller losses [Tri, 2015]:

- conduction loss: $R_{\text{eq}} I_0^2$
- switching loss: $(\alpha I_0 + \beta) V_{\text{bus}} + C f_{\text{eq}} V_{\text{bus}}^2$.

The total controller loss is

$$P_{\text{cl}} = R_{\text{eq}} I_0^2 + (\alpha I_0 + \beta) V_{\text{bus}} + C f_{\text{eq}} V_{\text{bus}}^2$$

where

- I_0 is the output current of the controller in A_{rms}
- V_{bus} is the bus voltage (battery voltage) of the controller
- R_{eq} is the equivalent resistance of the entire controller
- α is the linear component of the switching loss (per unit of bus voltage)
- β is the constant component of the switching loss (per unit of bus voltage)
- Cf_{eq} is the equivalent capacitance and frequency product of the entire controller
- $R_{eq} = 1.0800 \times 10^{2}$
- $\alpha = 3.3450 \times 10^{3}$
- $\beta = 1.8153 \times 10^{2}$
- $Cf_{eq} = 1.5625 \times 10^{4}$.

5 The Inductors

The Wave Sculptor 22 requires a minimum amount of inductance for each motor phase in order to operate properly [Tri, 2015]. In order to achieve this minimum amount of inductance a set of three inductors are provided with the motors to connect to the three phases of the motor in a series connection [Mar, 2013].

When used with a Wave Sculptor 22, the loss of one inductor can be approximated by [Mar, 2013]:

$$P_{il} = 12 \times 10^{3} \left(\frac{i}{2}\right)^{2} + 2.7 \times 10^{6} \left(\frac{i}{2}\right)^{3} \times 3.183\omega.$$

As with the controller, the dependence on torque τ comes from the currents i dependence on torque. And as we need three inductors per motor, the total loss will be three times this value. Figure 4 shows the inductor losses versus torque. Like the motor loss, the inductor losses increase at an increasing rate as torque increases.

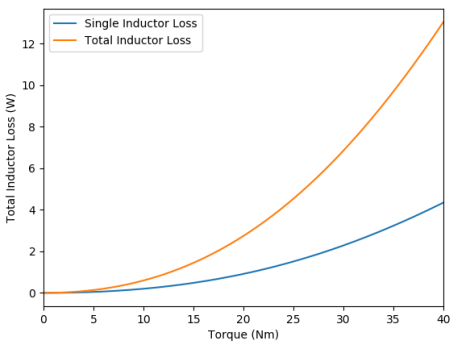

Figure 4: Inductor Losses

6 Total Losses

The total losses are the sum of the motor losses, the controller losses and the three inductor losses, and are a function of required torque τ:

$$f(\tau) = P_{\text{ml}} + P_{\text{cl}} + 3P_{\text{il}}.$$

Figure 5 shows how the total losses change with torque. Losses from the motor make up the majority of total losses. We also see from this graph that the losses appear to be increasing at an increasing rate, which suggests that the derivative of the losses is always increasing and the second derivative is always positive. Due to how the motor losses are calculated we don't have a simple formula for the total loss function or it's derivatives (although if we fix the number of iterations we could obtain a formula). However, using numerical approximation we can still calculate and graph the derivatives. Figure 6a shows the derivative of the total loss function and as expected it is always increasing. Likewise Figure 6b shows the second derivative of the total loss function which is always positive.

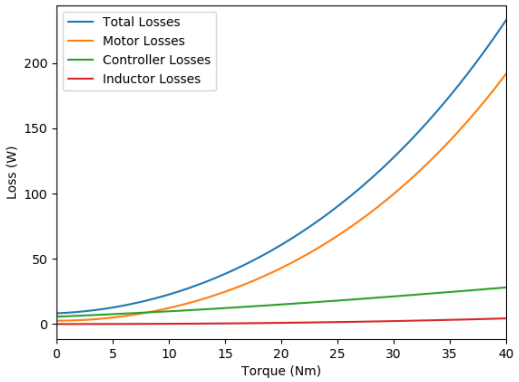

Figure 5: Total Losses

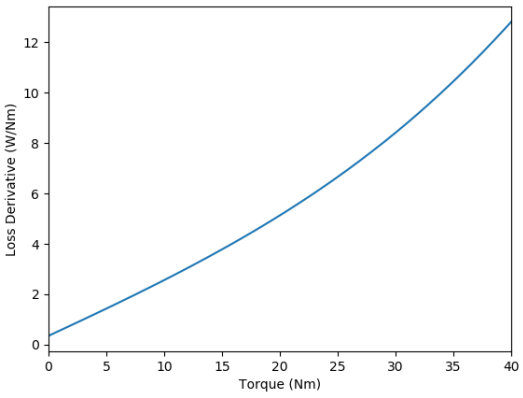

(a) Total Loss Derivative

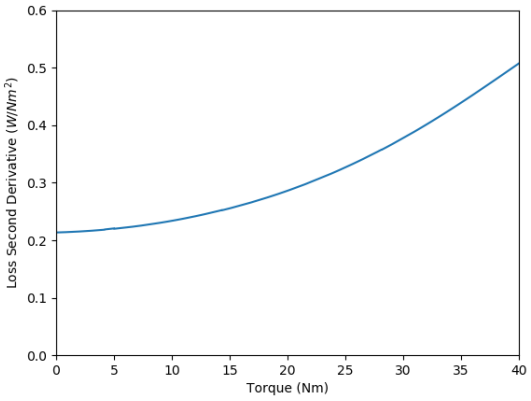

(b) Total Loss Second Derivative

Figure 6: Numerical Approximations of the Total Loss Function's Derivatives

At cruising speed, beside the required torque there are two other variables that may vary—the ambient temperature around the motors and the voltage of the battery. Figure 7a shows how total losses are related to the ambient temperature around the motor and Figure 7b shows how the total losses are related to the voltage of the battery.

Table 1 shows that losses increase with temperature, and as torque increases the percentage loss increases with torque. Table 2 shows that losses increase with bus voltage, but the percentage loss decreases with torque.

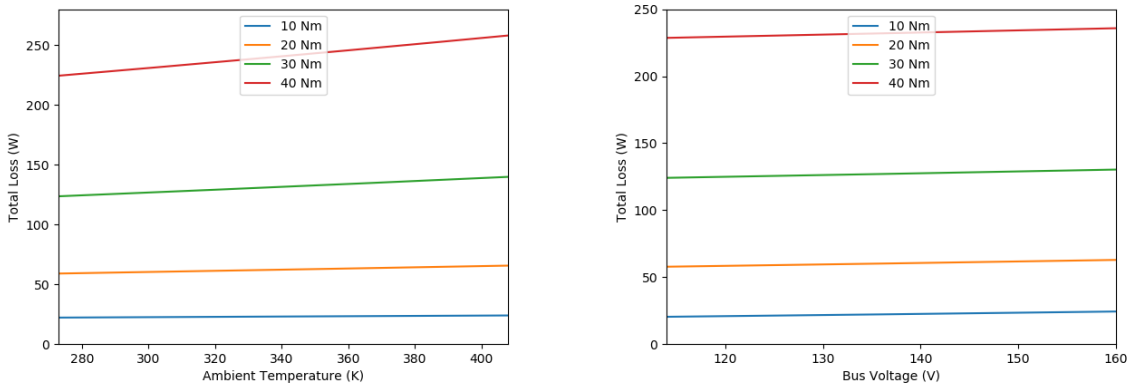

(a) How Loss Varies With Ambient Temperature

(b) How Loss Varies With Battery Voltage

Figure 7: How Loss Varies With Non-Torque Factors

Torque	Total Loss at 273 K	Total Loss at 408 K	Difference	Percent Increase
10 Nm	22.20 W	23.98 W	1.78 W	8.02 %
20 Nm	59.03 W	65.64 W	6.61 W	11.20 %
30 Nm	123.60 W	139.83 W	16.23 W	13.13 %
40 Nm	224.38 W	257.98 W	33.60 W	14.97 %

Table 1: Total Loss Values as Ambient Temperature Vary

Torque	Total Loss at 114 V	Total Loss at 160 V	Difference	Percent Increase
10 Nm	20.42 W	24.37 W	3.95 W	19.34 %
20 Nm	57.80 W	62.88 W	5.08 W	8.79 %
30 Nm	124.12 W	130.30 W	6.18 W	4.98 %
40 Nm	228.58 W	235.79 W	7.21 W	3.15 %

Table 2: Total Loss Values As Battery Voltages Vary

7 Optimal Power Split

7.1 Identical Motor and Controller Systems

Suppose the two motor and controller systems are identical. For a given battery voltage, speed and required torque, we want to determine the proportion of the required torque that should be supplied from each motor so that the total loss is minimised. The power loss from a single motor and controller is $f(\tau)$ for required torque τ. To find the optimal way to split the torque production we define the torque split function as:

$$g(\alpha) = f(\alpha\tau) + f\left((1-\alpha)\tau\right), \tag{1}$$

which describes the total loss from both motors and controllers for a required torque τ in terms of the proportion α of torque produced by one of the motor and controller systems, as $\alpha\tau$ will give the torque to be provided by one motor and controller system and $(1-\alpha)\tau$ will give the remainder of the required torque which is to be produced by the other motor and controller system. Figure 8 shows the optimal split function graphed for a variety of torques. From this graph it appears that the optimal solution is always $\alpha = 0.5$. We will show that not only is this the case for our motor and controller systems, it is also the case for many motor and controller systems. Figure 9 shows the differences in the losses from using one motor for all the torque versus splitting the torque equally between the motors, we see that in low torques this difference is relatively minor, but that the difference increases quickly at the higher torque values.

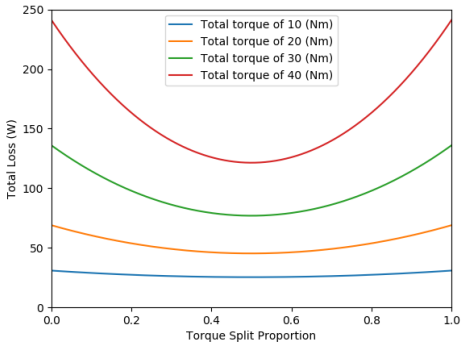

Figure 8: The Optimal Power Split Curves

What causes the equal split solution is that, as seen in Section 6, losses increase at an increasing rate as torque increases. This means that the first derivative of the total loss function is an increasing function, so that $a < b \implies f^{0}(a) < f^{0}(b)$, and that the second derivative of the loss function is always positive: $\forall x, f^{00}(x) > 0$.

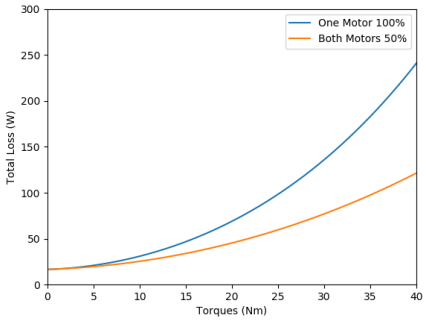

Figure 9: Losses From Using One Motor Versus Both Motors

To show that the equal split solution is optimal we take the derivative of the torque split function (Equation (1)):

$$g(\alpha) = f(\alpha\tau) + f\left((1-\alpha)\tau\right),$$
$$g'(\alpha) = \tau f'(\alpha\tau) - \tau f'\left((1-\alpha)\tau\right).$$

The torque split function has a stationary point when $g'(\alpha) = 0$:

$$0 = \tau f'(\alpha\tau) - \tau f'\left((1-\alpha)\tau\right)$$
$$\implies \tau f'(\alpha\tau) = \tau f'\left((1-\alpha)\tau\right)$$
$$\implies f'(\alpha\tau) = f'\left((1-\alpha)\tau\right),$$

which shows that the value of the derivative of one motor loss function has to equal the value of the derivative of the other's loss derivative. However, from before we know that this derivative is always increasing, $a < b \implies f'(a) < f'(b)$, which means this equality is only possible when the arguments are equal, giving us:

$$\alpha\tau = (1-\alpha)\tau$$
$$\implies \alpha = \frac{1}{2}.$$

This means that the torque split function has only one stationary point at $\alpha = \frac{1}{2}$. We can classify this is a minimum using the second derivative test. The second derivative of the torque split function is:

$$g''(\alpha) = \tau^2 f''(\alpha\tau) + \tau^2 f''\left((1-\alpha)\tau\right).$$

When the required torque $\tau > 0$ we also have that the second derivative of the motor loss functions is always positive, $\forall x, f''(x) > 0$. Therefore $g''(\alpha)$ is clearly always positive including for $\alpha = \frac{1}{2}$, which by the second derivative test for stationary points means that $g(0.5)$ is a minimum point.

Furthermore, as $g''(\alpha) > 0$ for all $\tau > 0$ and all $0 \leq \alpha \leq 1$, then $g(\alpha)$ is strictly convex meaning any local minimum is also the unique global minimum, meaning that the minimum point found at $\alpha = \frac{1}{2}$ is the only possible minimum point.

So we have found that the strategy that minimises losses in our dual in-wheel motor controller system is equally splitting torque production between the motors. However, this solution applies only if the two motor and controller systems have the exact same loss curves, which may not apply in general. In the next section we examine what happens if the two systems have different losses.

7.2 Non-identical Motors

We now consider the case where the second motor's loss function is some multiple of the losses of the first motor, so the first motor's losses will remain $f(\tau)$, but the second motor's losses will be $h(\tau) = \beta f(\tau)$. The torque split function becomes:

$$\begin{aligned} & g(\alpha) = f(\alpha\tau) + h\left((1-\alpha)\tau\right) \\ \implies & g(\alpha) = f(\alpha\tau) + \beta f\left((1-\alpha)\tau\right). \end{aligned} \tag{2}$$

Figure 10 shows the modified torque split function for several values of β. The optimal solution favours the more efficient motor one, but still stays relatively close to an equal split even with the second motor experiencing 25% extra losses ($\beta = 1.25$). Figure 11 shows the difference in losses using the new optimal split point versus reaming with an equal split; the difference is negligible for $\beta = 1.25$ and $\beta = 1.5$ and even for $\beta = 1.75$ and $\beta = 2$ (100% extra losses) the difference is quite small.

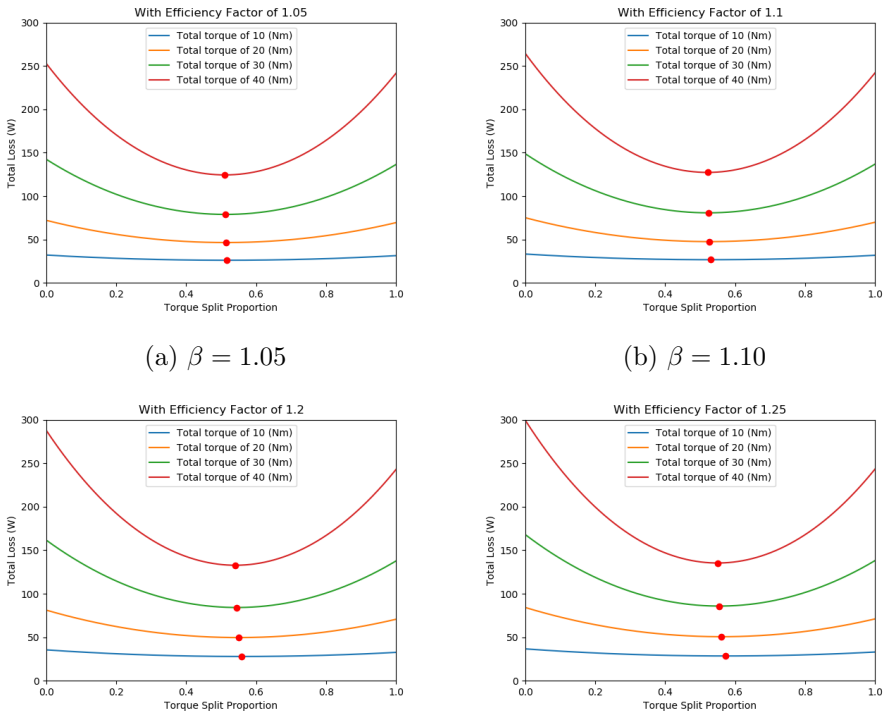

(a) $\beta = 1.05$ (b) $\beta = 1.10$

(c) $\beta = 1.20$ (d) $\beta = 1.25$

Figure 10: Power Split Curves When Second Motor Suffers Extra Loss

We can try to find where the new optimal solutions are using the stationary points as before, by starting with Equation (2) and taking its derivative:

$$\begin{aligned} g(\alpha) &= f(\alpha\tau) + \beta f\left((1-\alpha)\tau\right) \\ \implies g'(\alpha) &= \tau f'(\alpha\tau) - \beta\tau f'\left((1-\alpha)\tau\right). \end{aligned}$$

There is a turning point at:

$$\begin{aligned} 0 &= \tau f'(\alpha\tau) - \beta\tau f'\left((1-\alpha)\tau\right) \\ \implies \tau f'(\alpha\tau) &= \beta\tau f'\left((1-\alpha)\tau\right) \\ \implies f'(\alpha\tau) &= \beta f'\left((1-\alpha)\tau\right). \end{aligned}$$

Previously were we able to use the fact that the derivative was increasing to get a solution, but in that case we had the two values of the derivative exactly equal to each other. In this case the derivative of the loss of the the second motor has to be β times the derivative of the loss of the first motor. As we don't have a direct equation for the derivative, the optimal split point has to be solved numerically; we used a ternary search to find the optimal split point.

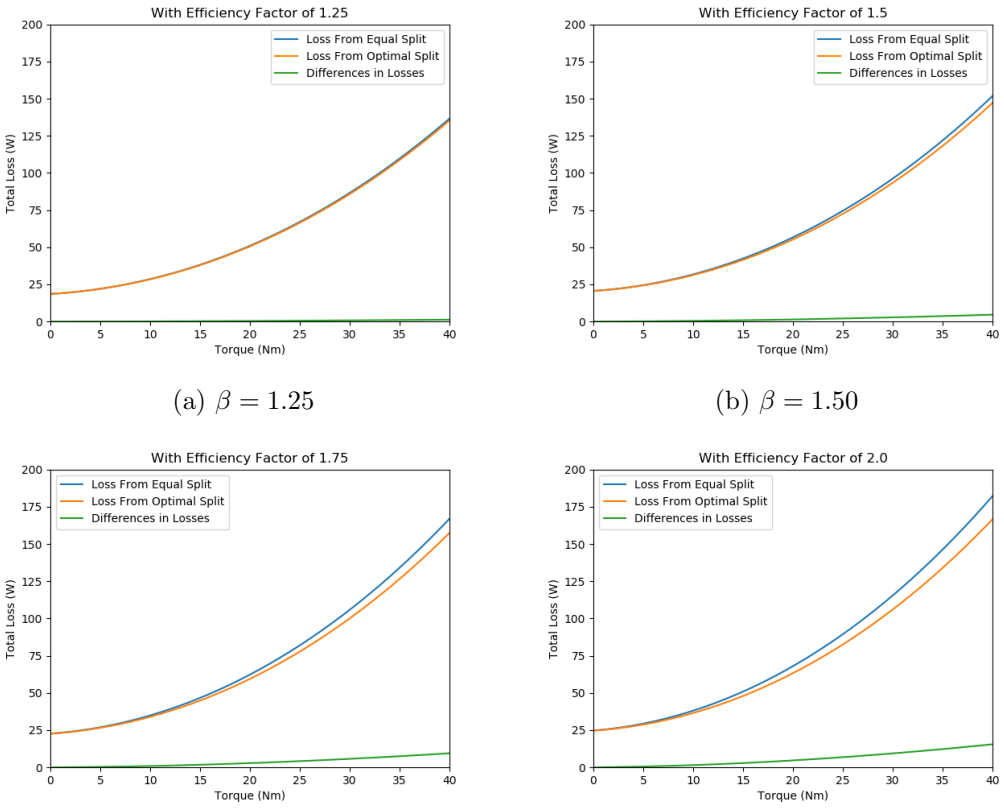

(a) $\beta = 1.25$ (b) $\beta = 1.50$

(c) $\beta = 1.75$ (d) $\beta = 2.00$

Figure 11: Optimal Loss Versus Equal Split Loss

Using the second derivative of the modified torque split function:

$$\begin{aligned} g'(\alpha) &= \tau f'(\alpha\tau) - \beta\tau f'\left((1-\alpha)\tau\right) \\ \implies g''(\alpha) &= \tau^2 f''(\alpha\tau) + \beta\tau^2 f'\left((1-\alpha)\tau\right), \end{aligned}$$

we find that like the original torque split function, it is always positive making this a strictly convex function when the required torque and β are both positive, meaning we always have one minimum point which is also the global minimum point. Therefore a ternary search will find the optimal split point.

So we have found that if the motors differ slightly the optimal torque split will be to favour the more efficient motor. However, we have also seen that the extra loss incurred when using an equal split solution is relatively small for our motors.

7.3 Final Strategy

We saw that if the motor and controller loss functions are exactly the same for both motors and loss increases with torque with increasing derivative that the optimal strategy is to distribute torque production equally among both motors. We also saw that the extra losses incurred from using equal torque distribution when there is a slight difference in the performance of our motors is not expected to be significant. So considering all these factors, the torque distribution strategy at cruising speed that makes sense is to always equally split torque production across both motors, which has the benefit of being simple to implement on a microcontroller as a real time strategy.

8 Related work

The literature contains some articles on the control of dual motors, but mostly concerns systems more complicated that the system that will be used by the solar car.

Jian et al. [2009] discuss optimal system efficiency for a multi-motor drive system for a bus. They note that while permanent magnet synchronous motors already have high efficiency, this efficiency depends on the methods used to control the motors. They suggest that an appropriate torque distribution strategy can improve the multi-motor drive system efficiency, and show that it is more efficient to use one motor under light load conditions, and to use both motors under heavy load conditions. They also show that dividing the torque evenly between motors is not necessarily the most efficient strategy, but they do not discuss the structure of the optimal solution.

Hu et al. [2015] propose a system using two motors with different powers, connected using gears and clutches. They use a sequential quadratic programming method to find the optimal power split for

different conditions, and store the results in a look-up table that can be used while driving. The optimisation of the efficiency gives the optimal torque motor 1 should be driven at, the optimal torque motor 2 should be driven at, the optimal speed motor 1 should be driven at and the optimal speed motor 2 should be driven at as function of the vehicle speed, the vehicle acceleration and the state of charge of the battery.

Tseng et al. [2015] describe online maximum efficiency tracking control for a dual-motor drive system. They do not model losses in the system. Instead, they measure the input power at the DC bus, measure the output power, and then vary the motor input torques to find the torque distribution that maximises efficiency. Two algorithms are proposed and compared: a steepest ascent algorithm and a fuzzy logic algorithm. They found that their fuzzy logic algorithm performed better, reaching a slightly better maximum efficiency and reaching the most efficient point quicker. Their control system operates on very small time scales of less then 0.1 seconds.

Zhang et al. [2015] use Pontryagin's principle to find necessary conditions for an optimal control strategy for a dual-motor-driven electric bus. Their drive system includes gears and clutches that introduce mechanical losses that we do not have.

Hu et al. [2018] propose a dual-motor powertrain system to improve the dynamic and economic performance of a pure electric vehicles. They consider a powertrain with a 22 kW motor and a 10 kW motor connected using a gear and clutch system that can operate in four modes: driving from motor 1, driving from motor 2, a torque combining mode, and a speed combining mode for high-speed operation. Overall efficiency is a function of transmission mode and the torque and speed of each motor. They use sequential quadratic programming to find the optimal mode and motor controls for various required vehicle speeds and torques, from which they develop a mode selection strategy that depends on the vehicle speed and required torque. Our system is simpler—we do not have a complicated transmission, and the speeds of the two motors are given.

Zhao et al. [2018] established a energy saving strategy for a dual motor system for an urban bus. They find an optimal torque ratio using the state of charge of the battery, the target torque and the target velocity using a dynamic programming solution, but the calculation is too slow for solving in real time. For on-road solutions, they pre-calculate solutions for different scenarios using their dynamic programming algorithm, then use a clustering algorithm to split these solutions in to separate clusters. The boundaries of the clusters are determined using a classification algorithm such as a support vector machine. Then, within each cluster, the actual points (torque split ratio, velocity, accelerator pedal position) were approximated by piecewise polynomials, and these polynomials used for on-road selection of strategy. The result was that the efficiency of the on-road strategy achieved is usually only 10% worse but can reach up to 95% of the dynamic programming strategy efficiency over a start-stop traffic cycle.

Da and Bo [2015] focused on optimising when a dual-motor system should switch from using one motor to using two motors. To do this they found the optimal driving force split between the two motors as a function of the vehicle speed and target driving force. They focused on identifying situations when all the driving force is supplied by one motor, compared to when the driving force is split between the two motors. Their problem differs from ours, as they used two different motors, one connected to the front axle and one connected to the rear axle with different gear ratios.

9 Conclusion and Discussion

This project was concerned with finding out how a solar car powered by two in-wheel motors should be controlled in order to minimise power losses in the motors and motor controllers.

Most of the previous research concerned much more complex systems than our in-wheel motors, and often used practical experiments to get exact measurements for the performance of the motors in order to create their control strategies. However the papers Zhao et al. [2018] and Da and Bo [2015] did provide the idea for solving the problem using the torque split ratio, representing the proportion of torque provided by motor one.

To solve the problem we investigated the power losses that occur in the ATN Solar Car's motor and controller systems. While there is not a simple formula for these losses, we were still able to analyse losses using algebraic, graphical and numeric methods. When cruising at a constant speed, motor and controller losses were minimised by splitting torque production equally among both motors.

A Motor Specifications

Table 3 contains the technical specifications of the motors. Table 4 contains the performance of the motors at its nominally rated speed and torque which is 111 rad/s and 16.2 Nm respectively. Table 5 contains the absolute maximum ratings for the motors. All these tables come from the manual for the motors [Mar, 2013].

Table 3: Motor Specifications

Property	**Value**
Number of poles	40
Number of phases	3
Mass of wheel motor	18.8 kg
Nominal speed	111 rad/s $\approx$ 1060 rpm
Nominal torque	16.2 Nm
Phase resistance	0.0575 Ω
EMF constant – L-N RMS EMF/speed	0.45 Vs/rad
Torque constant per phase	0.44 Nm/A

Table 4: Motor Performance at Nominal Rating

Property	**Value**
L-N RMS EMF	50 V
RMS phase current	12.3 A
Copper loss	25.9 W
Eddy Current Loss	2.6 W
Internal Motor Windage	2.1 W
Wheel Losses	25.1 W
Total loss	55.7 W
Output Power	1800 W
Efficiency	97.0 %
Nominal winding temperature rise	14 K
Overload winding temperature rise	70 K

Table 5: Motor Absolute Maximum Ratings

Property	**Value**
Maximum winding temperature	135 °C
Maximum speed	157 rad/s $\approx$ 1500 rpm
Maximum rated torque	80 Nm
Maximum continuous torque	42 Nm

References

W. Da and W. Bo. Research on driving force optimal distribution and fuzzy decision control system for a dual-motor electric vehicle. In *2015 34th Chinese Control Conference (CCC)*, pages 8146–8153, July 2015. doi: 10.1109/ChiCC.2015.7260936.

Jianjun Hu, Lingling Zheng, Meixia Jia, Yi Zhang, and Tao Pang. Optimization and model validation of operation control strategies for a novel dual-motor coupling-propulsion pure electric vehicle. *Energies*, 11(4), 2018. ISSN 1996-1073. doi: 10.3390/en11040754. URL http://www.mdpi.com/1996-1073/11/4/754.

M. Hu, J. Zeng, S. Xu, C. Fu, and D. Qin. Efficiency study of a dual-motor coupling EV powertrain. *IEEE Transactions on Vehicular Technology*, 64(6):2252–2260, June 2015. ISSN 0018-9545. doi: 10.1109/TVT.2014.2347349.

Zhang Jian, Wen Xuhui, and Zeng Lili. Optimal system efficiency operation of dual PMSM motor drive for fuel cell vehicles propulsion. In *2009 IEEE 6th International Power Electronics and Motion Control Conference*, pages 1889–1892, May 2009. doi: 10.1109/IPEMC.2009.5157704.

H. C. Lovatt, V. S. Ramsden, and B. C. Mecrow. Design of an in-wheel motor for a solar-powered electric vehicle. *IEE Proceedings - Electric Power Applications*, 145(5):402–408, Sept 1998. ISSN 1350-2352. doi: 10.1049/ip-epa:19982167.

Axial Flux Stub Axle Wheel Motor For Solar Vehicle Applications. Marand, April 2013.

Eric Forsta Thacher. *A Solar Car Primer: A Guide to the Design and Construction of Solar-Powered Racing Vehicles*. Springer, 2015.

WaveSculptor 22 Motor Drive User's Manual. Tritium, August 2015.

S. Tseng, T. Liu, J. Hsu, L. R. Ramelan, and E. Firmansyah. Implementation of online maximum efficiency tracking control for a dual-motor drive system. *IET Electric Power Applications*, 9(7): 449–458, 2015. ISSN 1751-8660. doi: 10.1049/iet-epa.2014.0415.

World Solar Challenge. 2019 world solar challenge: Overview, 2019. URL https://www.worldsolarchallenge.org/about_wsc/overview. [Online; accessed 22-January-2019].

Shuo Zhang, Rui Xiong, and Chengning Zhang. Pontryagin's minimum principle-based power management of a dual-motor-driven electric bus. *Applied Energy*, 159:370–380, 2015. ISSN 0306-2619. doi: 10.1016/j.apenergy.2015.08.129. URL http://www.sciencedirect.com/science/article/pii/S030626191501065X.

Mingjie Zhao, Junhui Shi, and Cheng Lin. Energy management strategy design for dual-motor coaxial coupling propulsion electric city-buses. *Energy Procedia*, 152:568–573, 2018. ISSN 1876-6102.

doi: 10.1016/j.egypro.2018.09.212. URL http://www.sciencedirect.com/science/article/pii/S1876610218307574. Cleaner Energy for Cleaner Cities.